Perspectives

CAMBRIDGE UNIVERSITY PRESS

Status and perspectives of the FUSION INFN project for the study and optimization of the $^{11}\mathrm{B}(\mathrm{p},\alpha)2\alpha$ nuclear fusion reaction for Inertial Confinement applications

Giuseppe Antonio Pablo Cirrone[1,2] ⓘ, Fabrizio Consoli[3,4], Nicolò Macaluso[1,5], Salvatore Mirabella[5,6] ⓘ, Farmesk Abubaker[1], Shubham Agarwal[7,8], Massimo Alonzo[3,4], Carmen Altana[1], Sahar Arjmand[1] ⓘ, Aldo Bonasera[1,9], Davide Bortot[10,11], Roberto Catalano[1], Michal Cervenak[12], Tomasz Chodukowski[13], Caterina Ciampi[11,14,15], Mattia Cipriani[3,4], Giacomo Cuttone[1], Pooja Devi[7,8], Edoardo Domenicone[3,16], Roman Dudzak[7,12], David Ettel[7], Francesco Filippi[3,17], Nunzia Gallo[18], Pavel Gajdos[12], Lorenzo Giuffrida[1,19], Benoist Grau[3,4,20], Luca Guardo[1], Mariacristina Guarrera[1], Ali Hassan[1,5], Valentina Iacono[5], Libor Juha[7], Josef Krasa[7], Michal Krupka[7,12], Miroslav Krus[12], Gaetano Lanzalone[1,21], Luciana Malferrari[22], Daniele Margarone[1,19], Gustavo Messina[1], Giovanni Morello[23,24,25], Massimo Nocente[11,16], Fabrizio Odorici[13], Libero Palladino[26], Alfio Domenico Pappalardo[1], Gabriele Pasquali[11,14], Giada Petringa[1], Antonino Picciotto[27,28], Tadeusz Pisarczyk[13], Angelo Maria Raso[4,20], Rosaria Rinaldi[23,29], Marcin Rosinski[13], Zofia Rusiniak[13], Luca Salvatore[18], Antonino Scandurra[5], Massimiliano Sciscià[3,4], Sushil Singh[7,12,30] ⓘ, Przemysław Tchórz[13], Antonio Trifiró[6,31], Salvatore Tudisco[1], Edmond Turcu[32,33] and Claudio Verona[4,20]

[1]INFN-Laboratori Nazionali del Sud, Catania, Italy; [2]Centro Siciliano di Fisica Nucleare e Struttura della Materia, Catania, Italy; [3]ENEA-Nuclear Department – Centro Ricerche Frascati, Frascati, Italy; [4]INFN – Section of "Tor Vergata", Roma, Italy; [5]Department of Physics and Astronomy, University of Catania, Via S. Sofia 64, Catania, Italy; [6]INFN – Section of Catania, Catania, Italy; [7]Institute of Physics, Czech Academy of Sciences, Prague, Czech Republic; [8]Faculty of Mathematics and Physics, Charles University, Prague, Czech Republic; [9]Cyclotron Institute, College of Science, Texas A&M University, College Station, College Station, TX, USA; [10]Polytechnic of Milan, Milan, Italy; [11]INFN – Section of Milan, Milan, Italy; [12]Institute of Plasma Physics, Czech Academy of Sciences, Prague, Czech Republic; [13]Institute of Plasma Physics and Laser Microfusion, Warsaw, Poland; [14]Department of Physics and Astronomy, University of Florence, Sesto Fiorentino, Italy; [15]Grand Accélérateur National d'Ions Lourds (GANIL), CEA/DRF–CNRS/IN2P3, Caen, France; [16]Department of Physics "G. Occhialini", University of Milano-Bicocca, Milan, Italy; [17]INFN – Laboratori Nazionali di Frascati, Frascati, Italy; [18]Department of Engineering for Innovation, University of Salento, Lecce, Italy; [19]ELI Beamlines Facility, The Extreme Light Infrastructure ERIC, Dolni Brezany, Czech Republic; [20]Department of Industrial Engineering, University of "Tor Vergata", Rome, Italy; [21]Faculty of Engineering and Architecture, University of Enna "Kore", Enna, Italy; [22]INFN – Section of Bologna, Bologna, Italy; [23]INFN – Section of Lecce, Lecce, Italy; [24]CNR IMM – Institute for Microelectronics and Microsystems – University of Lecce, Lecce, Italy; [25]Center for Biomolecular Nanotechnologies, University of Lecce, Istituto Italiano di Tecnologia, Arnesano (LE), Italy; [26]INFN – Section of L'Aquila, L'Aquila, Italy; [27]Micro Nano Facility, Sensors and Devices Centre, Fondazione Bruno Kessler, Trento, Italy; [28]INFN – Trento Institute for Applied Science, Trento, Italy; [29]Department of Mathematics and Physics "Ennio De Giorgi", University of Lecce, Lecce, Italy; [30]Faculty of Electrical Engineering, Czech Technical University in Prague, Prague, Czech Republic; [31]Department MIFT, University of Messina, Messina, Italy; [32]UKRI/STFC Central Laser Facility, Rutherford Appleton Laboratory, Harwell Campus, Didcot, UK and [33]ELI-NP, Extreme Light Infrastructure – Nuclear Physics, Magurele-Bucharest, Romania

Abstract

The FUSION project (an acronym for FUsion StudIes of prOton boron Neutron-less reaction in laser-generated plasma) was launched in 2022 by researchers from INFN (Istituto Nazionale di Fisica Nucleare) and ENEA. This project marks the first scientific initiative funded by INFN in

the field of Inertial Confinement Fusion (ICF). The main objectives of FUSION are to develop a new generation of solid targets designed to enhance the $^{11}B(p, \alpha)2\alpha$ fusion reaction rate, being this reaction a potential candidate for future ICF schemes. FUSION will also focus on designing novel diagnostic techniques for measuring reaction products and, ultimately, estimating alpha and proton cross-sections in a plasma environment.

The project will be carried out through two experimental campaigns at a laser facility equipped with a high-energy, long-pulse (picosecond) laser. In the proposed experimental setup, the $^{11}B(p, \alpha)2\alpha$ reaction will be triggered simultaneously 'in target' by the protons generated in the laser matter interaction and ^{11}B present in the same expanding plasma and in the 'pitcher-catcher' configuration. In FUSION, a set of measurements will also be dedicated to a first estimation of the proton and alpha-stopping power in a plasma. FUSION will enable a comprehensive understanding of the reactions and will help in optimize the conditions for future applications in inertial nuclear fusion with the $^{11}B(p, \alpha)2\alpha$ reaction.

Introduction

The conventional route of nuclear fusion for power generation is today mainly based on the reaction between deuterium and tritium nuclei, which yields one α-particle and one neutron: D+T $\rightarrow$ α (3.5 MeV) + n (14 MeV). However, this method presents significant technological challenges, including the production and handling of tritium, as well as the radiation damage and induced radioactivity caused by high-energy neutrons in the reactor. In this regard, the nuclear reaction between proton and the ^{11}B isotope, yielding three energetic α-particles, is very attractive, as it only involves abundant and stable isotopes as reactants and no neutrons in the reaction products. Since 2005 the $^{11}B(p, \alpha)2\alpha$ fusion has been effectively induced by means of high-power lasers (Ref [1]). In this case, an impressive and not completely explained progression in the reaction yield has been observed to the extent that the reaction has become of interest to the energy sector, where it is being considered in some cases as an alternative approach to conventional Inertial Confinement Fusion (ICF) schemes (Ref [2]). The FUSION (**FU**sion **S**tud**I**es of pr**O**ton boron **N**eutronless reaction in laser-generated plasma) project is an INFN (Istituto Nazionale di Fisica Nucleare, Italy) initiative that was launched in 2022 by INFN and ENEA (Agenzia nazionale per le nuove tecnologie, l'energia e lo sviluppo economico sostenibile, Italy) researchers for realizing a new generation of solid targets, with the purpose to enhance the $^{11}B(p, \alpha)2\alpha$ reaction rates, study new diagnostic approaches for the reaction products measurement and experimentally estimate alpha and proton stopping powers in a plasma environment. In this paper, the status and the first achievements reached within the FUSION project will be reported. The overview of the status and progress related to the $^{11}B(p, \alpha)2\alpha$ fusion studies in plasma in the framework of the ICF will be briefly discussed in Section 2. The main activities of FUSION and its Work Packages are detailed in Section 3. A description of the first experiment, conducted within FUSION and performed at the PALS facility (Prague, CZ), is provided in Section 4. The development status of new targets, designed to enhance fusion reactions and intended for use in the PALS experimental campaigns, is discussed in Section 5.

2. Role and interest of the $^{11}\text{B}(p, \alpha)2\alpha$ reaction in plasma

Over the last decades, the global energy crisis and the increasing demand for sustainable energy resources have stimulated the scientific community to intensify research on nuclear fusion for energy application. Two main approaches have been considered in this quest: Magnetic Confinement Fusion (MCF) and ICF (Ref [3]).

In particular, ICF is an energy production approach that initiates nuclear fusion by compressing and heating a target containing thermonuclear fuels, typically deuterium and tritium. The compression process brings the fuel to over 1000 times the density of solid within a short time frame, in the order of a few nanoseconds. This process is done to let the atoms overcome their mutual Coulomb repulsion and start to fuse. These high densities are achieved by imploding spherical shells (few millimetres in diameter) with high-power radiation from an external driver, such as X-rays, ion beams or high-power laser radiation (Refs [2, 4]).

Interest in ICF has surged following a major breakthrough at the National Ignition Facility (NIF) at Lawrence Livermore National Laboratory (LLNL) in the USA, where, in August 2021, researchers successfully converted 70% of the laser energy into the products of deuterium–tritium (DT) fusion reactions, achieving the so-called burning plasma condition (Ref [5]). In December 2022, NIF reported another milestone: for the first time globally, the fusion energy
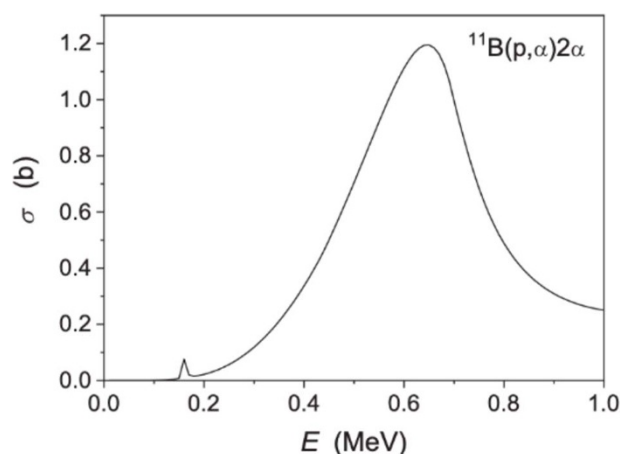
Figure 1. Classical (not in-plasma) $^{11}B(p,\alpha)2\alpha$ fusion reaction channel cross-section as a function of the incident proton energy in the laboratory reference framework (Ref [21]).

avoid neutron emissions as primary reaction products. Among these neutron-less reactions, the $^{11}B(p,\alpha)2\alpha$ reaction is especially promising. It has a positive Q-value of 8.7 MeV, producing only alpha particles without neutron byproducts (Ref [2]). These characteristics make $^{11}B(p,\alpha)2\alpha$ an attractive candidate for future fusion reactors, as evidenced by the interest from private companies like Marvel Fusion (Ref [10]) and HB11 Energy (Ref [11]) and others.

Seeing the increasing interest in this sector, different scientific initiatives, such as the European COST Action PROBONO (Ref [12]), have been developed to enhance knowledge of the laser-triggered proton–boron reaction. Experimentally, since 2005, the high cross-section of the p(^{11}B, α)2α reaction (Refs [13–15]) (see Figure 1) has enabled researchers to initiate a significant number of nuclear reactions by directing high-energy lasers at targets containing both boron and hydrogen (Ref [15]). Several groups (Figure 2) have tried different laser-driven approaches, set-ups and target materials, in order to characterize the reaction products (Ref [16]) and improve the alpha yield of the reaction demonstrating the possibility to reach up to 10^{10} particles/sr/shot (Refs [14, 15, 17–22]).

The most important challenges addressed in experiments involving the $^{11}B(p,\alpha)2\alpha$ fusion reaction are:

output exceeded the total energy input from the lasers by approximately 50%, resulting in a target gain greater than one (Refs [6–8]).

These landmark achievements were attained with an indirect drive approach (Ref [3]), consisting in the conversion of laser energy into X-ray radiation, to initiate the fusion. However, the employment of DT fuel presents significant technological and sustainability challenges, including the unavailability of tritium on Earth (tritium can be bred from lithium irradiated with neutrons) and high levels of neutron-induced radioactivity in the reactor structure (Ref [9]).

Consequently, the scientific community is exploring alternative, neutron-less fusion reactions, often referred to as the 'Holy Grail' for future, third-generation fusion power plants. Such reactions, unlike D-T fusion, do not require radioactive reagents (such as tritium), and instead rely on abundant natural reagents, and

(1) the capability to accurately characterize the laser–matter interaction and quantify the resulting fusion products;
(2) the ability to develop and characterize new target materials able to optimize the reaction rate;
(3) a thorough understanding of the underlying physics of the reaction within a plasma environment.

These topics represent the primary focus areas of FUSION, whose main goals, organization and results will be described in the following sections.
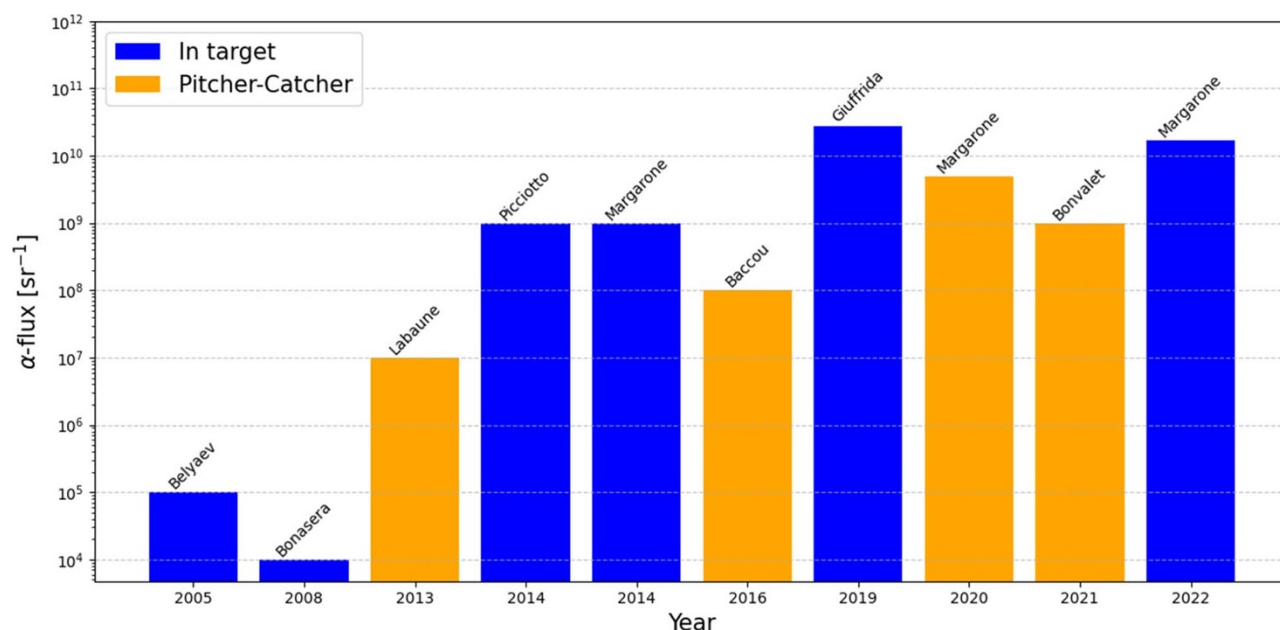

Figure 2. The maximum alpha particle yield per year for laser-driven fusion experiment, for both pitcher-catcher and in-target irradiation geometry.

3. The FUSION project and its main activities

The FUSION project is structured into four Working Packages (WPs), each focusing on specific aspects of plasma-based fusion research. WP1 is dedicated to studying fusion reactions in plasma, with the primary objective of enhancing alpha particle production. WP2 aims at investigating the interaction of protons and ions with borated plasma to achieve a deeper understanding of charged particle dynamics in plasma environments. WP3 focuses on the design, development and optimization of innovative targets to maximize the fusion reaction rate, while WP4 concentrates on the development of advanced diagnostic techniques for precise analysis of reaction products in plasma-based fusion. Together, these WPs address the core goals of the project, ranging from improving the efficiency of fusion reactions to advancing diagnostic methodologies.

The FUSION projects include 10 INFN sections, five Italian universities, the Polytechnic Universities of Milan and Turin, the 'Fondazione Bruno Kessler' and the ELI-Beamlines Institute in the Czech Republic (CZ). Each participant brings unique expertise and fulfils specific roles, contributing to the project's multidisciplinary approach. The primary aim of FUSION is to study the $^{11}B(p, \alpha)2\alpha$ fusion reaction channel in laser-generated plasmas, exploring its potential for a wide range of energetic and multidisciplinary applications. To achieve this, the project has three main objectives. The first is to maximize the reaction rate in plasma, which will be pursued by WP1 through studies of laser–plasma interactions using innovative targets developed in WP3. The second objective is to develop advanced diagnostic tools to measure the reaction rate by detecting the alpha particles and protons produced during the process, a task undertaken in WP4. Finally, the third objective is to deepen the understanding of the physics underlying the observed reaction rate. This will involve WP2 studying the interaction of protons and alphas, generated by conventional accelerators, with an expanding borated plasma.

3.1. Study of the $^{11}B(p, \alpha)2\alpha$ fusion reaction channel in plasma

The study and optimization of the $^{11}B(p, \alpha)2\alpha$ reaction in plasma will be conducted through experimental campaigns that will be performed using the high-energy, long-pulse PALS (Prague Asterix Laser System) laser, whose characteristics are summarized in Table 1.

These experiments will focus on studying the $^{11}B(p, \alpha)2\alpha$ reaction in two configurations: 'in-plasma' and 'pitcher-catcher', within the same laser shot, utilizing the developed targets. The 'in-plasma' configuration refers to scenarios where fusion reactions occur directly within the target irradiated by the main laser pulse. In this setup, protons and ^{11}B isotopes are accelerated inside the energetic and expanding plasma generated by the laser–target interaction. In contrast, the 'pitcher-catcher' configuration involves fusion reactions induced by protons exiting the primary target and striking a secondary boron target positioned along the normal axis of the primary target.

This approach allows for a direct comparison of fusion reaction rates under different conditions within the same laser shot. Specifically, it enables quantification of the difference between fusion reactions occurring in the plasma and those in a standard 'pitcher-catcher' scenario, where protons interact with a cold, solid boron target. The experimental set-up is depicted in Figure 3, which shows a CAD rendering of the interior section of the PALS interaction chamber. The laser pulse (illustrated as a green cone)

Table 1. PALS laser specifications (Ref [23])

General	
Fundamental wavelength	1.315 µm
Pulse duration	200–350 ps
Pulse contrast (prepulses & ASE)	$\sim 10^{-7}$
Repetition shot rate	25 min
Output energy stability (over 10 shots)	$< \pm 1.5\ \%$
Main beam	
Pulse energy at 350 ps	1 000 J
Pulse power at 350 ps	3 TW
Diameter	290 mm
Conversion efficiency to 3ω	55 %
Auxiliary beam	
Pulse energy at 350 ps	100 J
Diameter	148 mm
Conversion efficiency to 3ω	30 %

will be focused onto a thick solid target (yellow cylinder) using a focusing lens. This target, inclined at a 25° angle relative to the laser main axis, is composed of hydrogen and ^{11}B. Upon interaction with the laser, the solid target will transit into a plasma state, potentially initiating the $^{11}B(p, \alpha)2\alpha$ fusion reaction in the 'in-plasma' configuration. A portion of the protons accelerated during the laser–target interaction will propagate along the target normal axis and strike a secondary target, which is mounted on a dedicated holder. The secondary target consists of a natural boron slab, measuring 2 × 2 cm and 2 mm in thickness. If protons have sufficient kinetic energy, they will interact with the boron, triggering the $^{11}B(p, \alpha)2\alpha$ reaction and producing alpha particles, as part of the 'pitcher-catcher' configuration. The alpha particles generated will be detected using a CR39 track detector housed in a dedicated holder (highlighted in blue in Figure 3). To analyse the energy spectra of the emitted alpha particles, aluminium filters of varying thicknesses (ranging from 0 to 35 μm) will be placed in front of each detection aperture in the CR39 detector. In the experiments, time-of-flight diagnostic systems will also be employed, utilizing diamond and silicon carbide detectors positioned at various angles with respect to the normal of the primary target. The set-up will include three individual diamond detectors, one silicon carbide detector and a matrix of six diamond detectors. The effective detection areas of the detectors range from 1 to 6.5 mm². In particular, the diamond matrix is composed of six detectors, each with an active area of 6.3 mm², resulting in a total effective detection area of 37.8 mm². Filters with a thickness of 6 μm will be placed in front of the ToF detectors, while a set of filters ranging from 3 to 25 μm will be placed in front of the matrix detectors. The use of aluminium absorber serves to block low-energy ions and to separate the contribution of alpha particles. Additionally, for the detection of alpha particles in a mixed-signal regime, an 'a posteriori' analysis based on signal deconvolution will be employed to accurately isolate the different contributions. This set-up was previously used during an earlier experimental campaign, whose analysis is still ongoing, and it will be adopted in upcoming experiments.
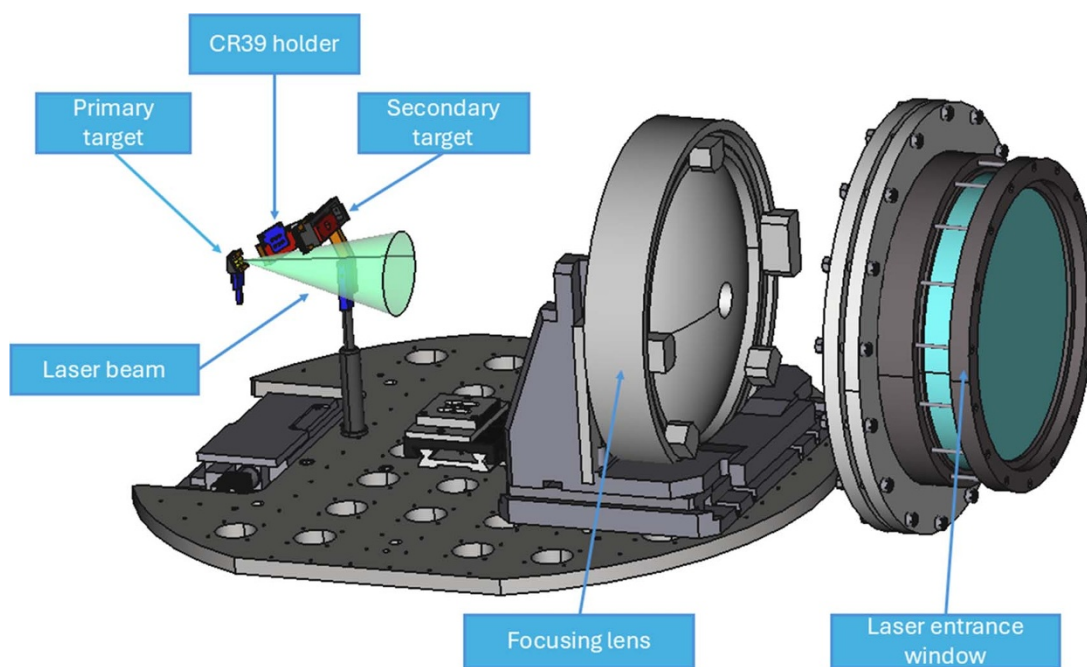
Figure 3. Layout of the experimental set-up that will be used for the study of the $^{11}B(p, \alpha)2\alpha$ reaction in a laser-generated plasma.
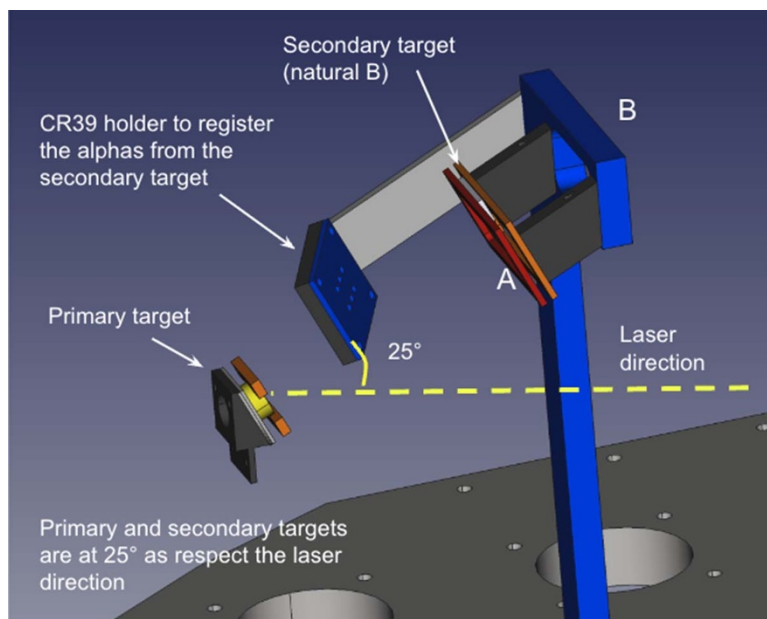

Figure 4. Rendering of the target system designed for the purposes of the FUSION experiments at the PALS facility.

A detailed view of the target system, including the primary target, the secondary target and the CR39 detector holder, is shown in Figure 4.

3.2. Study of the protons and alphas stopping power in a borated plasma

In FUSION, a set of measures will be dedicated to estimating the proton and alpha-stopping power in a borated plasma. In this case, a plasma will be generated in a vacuum using a 10 mJ, 6 ns laser pulse interacting with a solid target. After the initial expansion, the plasma plume will be characterized while, simultaneously, a synchronized proton or alpha microbeam from a conventional linear accelerator will cross it at the intersection point with the interferometer axis (Figure 5).

The energy loss of the traversing ions will be measured with a single event modality as a function of the plasma characteristics (temperature, density, etc.) by Time-of-Flight measurements and using Silicon Carbide detector as particles energy detectors. Alpha and proton beams will be provided by the 'Singletron' accelerators available at the Physics Department in Catania, Italy. A pulsed beam (bunch FWHM < 1 ns) will be obtained thanks to a chopper-bunching system funded, designed and realized within the FUSION project.

The determination of stopping power for ions within plasma entails a meticulous examination of single-particle interactions
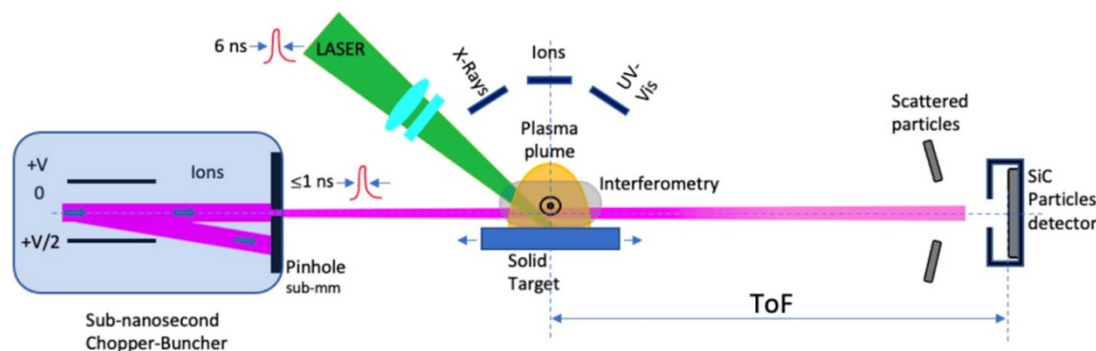
Figure 5. Experimental set-up for the proton and alpha stopping power measurements in a borated plasma. A 6 ns laser pulse generates a plasma plume that is crossed by a sub-nanosecond bunched ions beam. Energy loss in the plasma will be measured in single particle mode by silicon-carbide detectors.
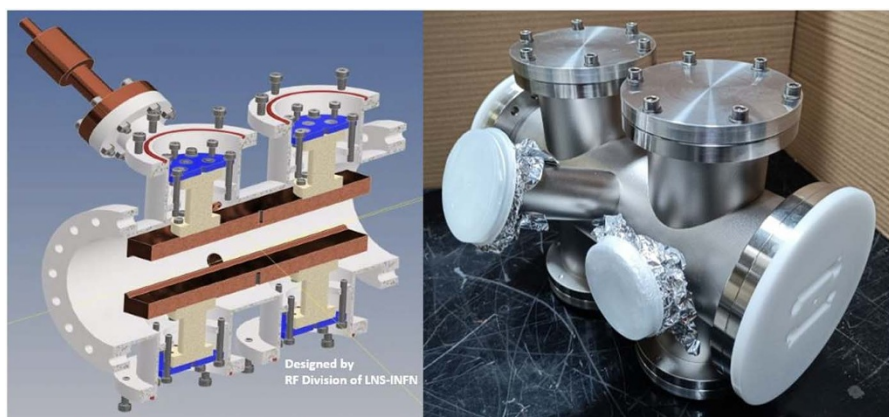

Figure 6. Left picture: mechanical design of the chopper-bunching system as defined during the first year of the FUSION project. Right: bunching system vacuum chamber delivered, assembled and ready to be installed in the experimental area.

within a well-defined plasma state. To achieve this, the development of a chopper-bunching system is imperative, enabling the controlled delivery of one or a few particles at a time with a temporal resolution of approximately 1 ns. This system will rely on a rapid electrostatic deflection mechanisms to manipulate particle beams crossing a pinhole. Initially, the continuous beam emitted by the Singletron undergoes bending via a switching magnet, followed by collimation to better define the beam emittance. Subsequently, the beam is deflected through a pair of electrodes and ultimately selected by a small collimator. The mechanical structure of the chopper has been designed (left side of Figure 6) and the whole system has then been simulated to evaluate both beam dynamics and time resolution. The mechanical sections of the bunching system have been manufactured, delivered and finally assembled as shown in Figure 6 (right side). The system is now ready to be installed along the Singletron experimental beamline of the Physics Department of Catania University (Italy) and the preliminary measurements are planned in 2025.

4. Ion diagnostics of the FUSION project

The FUSION project envisaged the development of a set of diagnostic tools dedicated to improving the detection of the reaction products. Time of flight (TOF) detectors (based on CVD synthetic diamonds and Silicon Carbides), Ion Collectors, Thomson-like spectrometers, interferometric and neutron detection systems will be developed to fulfil the needs of the experimental activities carried out in WP1 and WP2.

In this paper, we will, in particular, describe the development of two new detectors that are designed to obtain a better discrimination between the two main species produced in the $^{11}B(p,\alpha)2\alpha$ fusion reaction: the protons, directly generated by the laser–target interaction and the alphas, generated by the occurrence of the nuclear reaction. The two detectors are a matrix of synthetic diamonds (see Section 4.1) and an optimized version of a Thomson ion spectrometer (see Section 4.2).

4.1. The diamond matrix

A TOF detector matrix, composed of six diamond-based detectors in a sandwich configuration (metal/intrinsic diamond/metal), was developed and fabricated at the University of Rome 'Tor Vergata'. The detectors feature a high-purity intrinsic diamond layer grown homoepitaxially on a single-crystal diamond substrate using microwave-enhanced chemical vapour deposition. The intrinsic CVD diamond layer was precisely laser-cut from the substrate, achieving a thickness of 35 μm. Such thickness was selected to optimize the temporal resolution and ensure the complete absorption of protons up to 2.5 MeV and alpha particles up to 10 MeV. The detectors were assembled on a PCB board with an integrated bias-tee (R = 1 MΩ, C = 1 μF) and housed within an aluminium casing mounted on a KF-100 vacuum flange to shield against electromagnetic pulse (EMP) noise (see Figure 7-left). Six aluminium filters of varying thicknesses, i.e. 3, 6, 15, 18, 20 and 25 μm, were positioned in front of the detectors. The differing stopping powers of Al filters allow for enhanced analysis of particle
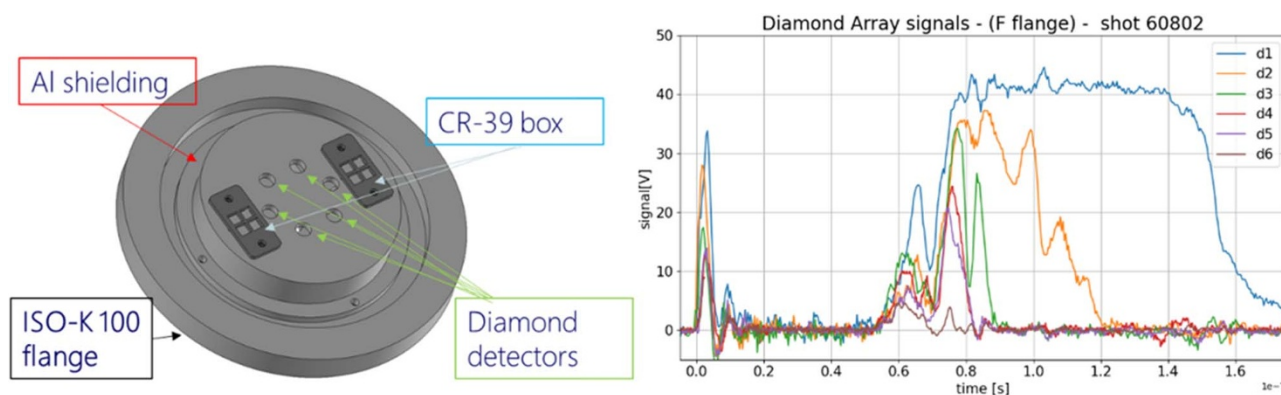
Figure 7. Left: aluminium shielding flange with CR39 and Diamond detectors inserted. Right: typical ToF signals from Diamond detector array with different aluminium filters applied.

energy spectra by distinguishing particles based on their mass and energy (Ref [24]). Additionally, the set-up includes two slots for CR-39 solid-state detectors, mounted on the inner side of the flange with identical Al filters, enabling comparative measurements. The TOF diamond matrix was successfully used to study and characterize the $^{11}B(p, \alpha)2\alpha$ reaction in plasma during the first experimental campaign at the PALS facility (see 3.1). The device was positioned at 53° relative to the target normal direction and placed 107 cm away from the target. The outputs were connected to a fast oscilloscope via six double-shielded RG223 cables. Figure 7-right shows a typical example of ToF signals captured by the TOF diamond matrix during the laser-target interaction. The figure clearly displays a distinct, narrow photopeak, which marks the starting point for the ToF measurement. Following this, a broader signal is visible, representing protons and ions with varying energies as they reach the detector. Signals from the detectors with different filters exhibit a noticeable reduction in both amplitude and time, demonstrating the system's effectiveness in differentiating and analysing the reaction products.

4.2. Thompson spectrometer

Within the FUSION project, we developed a diagnostic device, dedicated to the detection of alpha particles, that is based on Thomson spectrometry (i.e. a well-established method for revealing and differentiating accelerated protons and heavy ions in laser-plasma experiments). This device is capable of retrieving information on the proton spectrum and the spectrum of heavy ions, discriminating particles according to their mass-to-charge ratio A/Z. The alpha particles, generated by the $^{11}B(p, \alpha)2\alpha$ fusion reaction, will be detected on the A/Z=2 parabolic curve. However, the alpha particles must be differentiated from the other heavy ions with A/Z=2 generated in the laser-plasma interaction, especially C^{6+}, which are a common product when intense laser pulses interact with solid targets. This requires a high sensitivity of the device and/or additional discrimination techniques. Since one of the major challenges of alpha particle detection in $^{11}B(p, \alpha)2\alpha$ experiments is represented by the low particle flux (Ref [17]), this device has been designed, aiming at a high sensitivity and at the possibility to be implemented in proximity to the laser-plasma interaction point (Ref [18]). Taking inspiration from the Thomson Spectrometer (TS) prototypes developed by ENEA in the last years (Ref [25]), it features ad-hoc shielding case for the strong EMP generated inside the interaction chamber and the ionizing radiation, which interfere with the magnetic and electric field of the device and are typically responsible for the background noise on the device detector, respectively. The schematic of the device is reported in Figure 8A. The parameters are conceived for allowing proton detection at an energy from hundreds of keV, up to several MeVs for protons and similarly for alpha particles produced by $^{11}B(p, \alpha)2\alpha$, and have been optimized by numerical simulations (electromagnetic simulations and particle tracking). The deflecting dipole features a magnetic field of ≈ 400 mT and an electric field of >1 MV/m. The dipole geometry has been dimensioned for avoiding electrical breakdown even at multiple kV voltage. The simulated deflection of ions with A/Z=1 and A/Z=2 (see Figure 8A) indicates enough energy resolution for allowing the implementation of differential filters on a spatial scale of a few millimeters (Ref [26]), in the energy range that is typical for the alpha particles produced by $^{11}B(p, \alpha)2\alpha$ fusion reactions. The position of the detector inside the device will be adaptable by using an extension of the drift space after the deflecting dipole, allowing a further enhancement of energy resolution and magnification of the obtained parabolic traces (see Figure 8C). Moreover, the detector plane will be equipped with special frames for implementing single or multiple CR39-arrays (shown in Figure 8B), allowing a more detailed discrimination of the fusion reaction products. The device is currently at the assembly phase and will be tested during an experimental session planned for 2025.

5. Development of new targets

The third WP within the FUSION project is exclusively focused on the design, production and optimization of solid borated targets essential for investigating the 'in-plasma' $^{11}B(p, \alpha)2\alpha$ fusion reaction (WP1) and quantifying the stopping power within a plasma environment (WP2).

Five different target families are under development, each with specific physical and chemical characteristics. All the targets are designed to work with long-pulse lasers with characteristics similar to those reported in Table 1.

5.1. Borated pills from University of Catania

5.1.1. Targets chemical formulation

The targets consist of disks 13 mm in diameter, with thickness of 3 mm. Targets of reference (only resin) and resin+boron, were prepared. The resin+boron targets were obtained by using a mixture
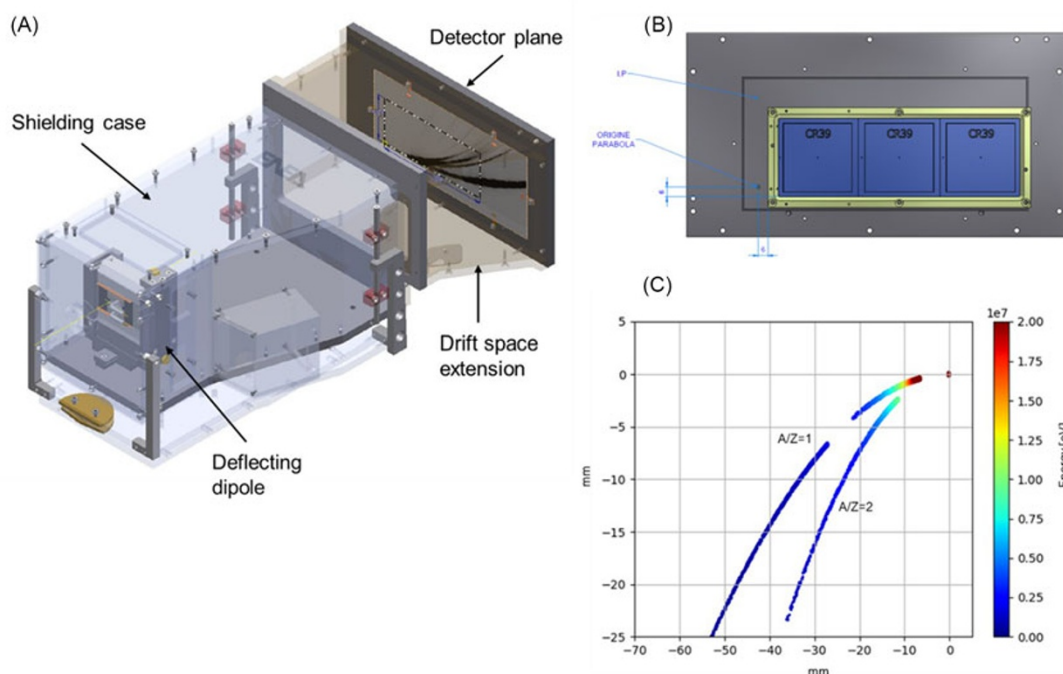
Figure 8. A. Schematic design of the alpha particle detection device. **B.** Improved design of the detector plane, allowing the use of a CR39 array. **C.** Parabolic traces of the deflected ions, computed by a particle tracking simulation, at the end of the drift space after the deflecting dipole (i.e. at the position of the particle detector of the device).
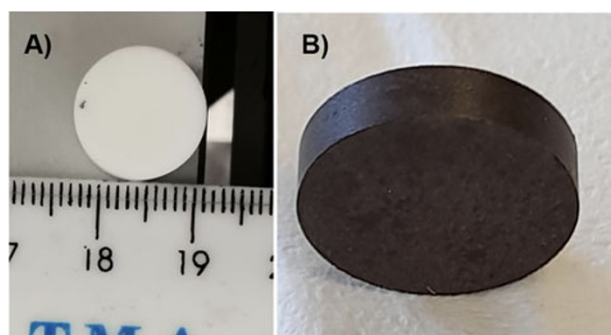

Figure 9. Pictures of the target pills (13 mm in diameter and 3 mm thin). **A.** Reference sample (only resin) and **B.** B50 sample (resin + elemental boron, at 2:1 wt. ratio).

Figure 10. Low-resolution optical micrographs of: **A.** reference and **B.** resin/boron 2:1 wt. target; **C.** and **D.** corresponding high-resolution SEM micrographs.

powder (2:1 wt. ratio) of: i) solid acrylic resin (Henry Schein Krugg, Italy, code 413004937) and ii) elemental amorphous boron (Sigma Aldrich Merck, Italy code 15580, with a purity ≥95%). The grain size of the elemental boron used was less than 1 μm, while that of the acrylic resin was a few tens of microns. Each target pill was prepared using about 0.420 g of the resin powder (for the reference sample) or of the mixture powder (B50 target sample). The powders were placed into a pellet die of 13 mm in diameter and added with 250 μL of liquid resin (Henry Schein Krugg, Italy, code 413004938), obtaining pastes. Furthermore, the pastes were pressed at 0.5 GPa for 10 minutes at room temperature. During this step the polymerization of the resin occurs. Figure 9 shows the pictures of the target pills of reference and B50 samples, respectively.

5.1.2. Characterization techniques

The scanning electron microscopy (SEM) was used for the characterization of the pill surface morphology. The SEM pictures
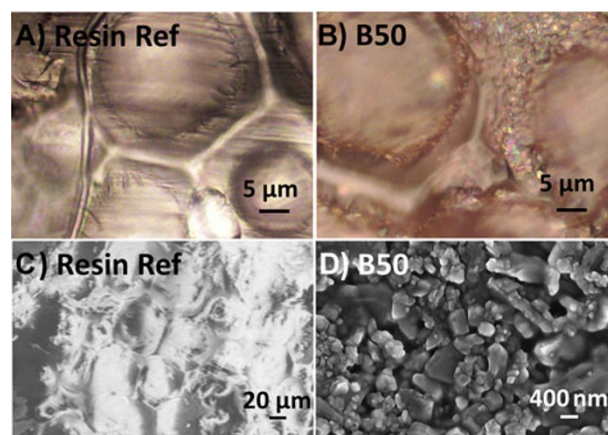
were obtained by a SEM Gemini Field Emission SEM Carl Zeiss SUPRATM 25 (FEG-SEM, Carl Zeiss Microscopy GmbH, Jena, Germany) set to the in-lens mode. An acceleration voltage of 5 keV and a working distance of 7 mm were used. Raman characterizations were obtained by a Horiba Scientific instrument model 1024 × 256-OE, equipped with a He–Ne laser model HNL225R, by THORLABS Inc. (43 Sparta Ave, Newton, New Jersey, U.S.A.), operating at a wavelength of 632.8 nm.

The surface of the reference target, visible from optical micrograph of Figure 10A and SEM of Figure 10C, shows the presence of insulating grains, bound together, which have dimensions of several micrometers. This morphology reflects the grain size of the solid acrylic resin which is, in fact, tens of micrometers large. The optical and SEM micrograph of the surface of the B50 target
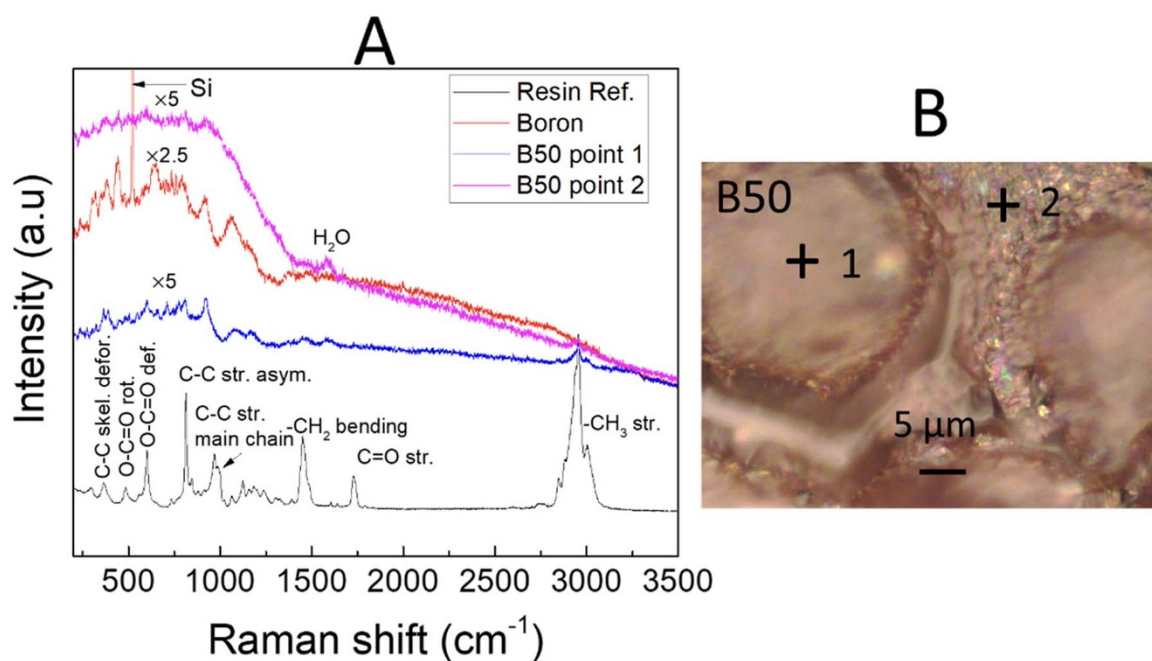
Figure 11. A. Raman spectra of boron (red line), resin (black line) and B50 target acquired at points 1 and 2 in the picture B (blue and magenta). The Si peak is due to the substrate used for the analysis of boron powder; **B.** corresponding optical micrograph of the points 1 and 2.

(Figure 10B and D) show the boron particles with an average size of less than 1 μm, mixed with the resin particles, which have much larger dimensions. This latter data are visible in the optical microscopy of Figure 10B.

Figure 11A shows the Raman spectra of boron alone (red line) and resin alone (black line). The spectrum of boron shows the peaks centred at 1067, 915, 801, 656, 431, 387 and 317 (cm^{-1}) that can be attributed to a mixture of amorphous boron and α-B and γ-B phases (Refs [27, 28]). The spectrum of the resin shows the peaks assigned to -CH$_3$ stretching (2954 cm^{-1}), C=O stretching (1728 cm^{-1}), –CH$_3$ symmetric bending (1462 cm^{-1}), C–C stretching of the main chain (970 cm^{-1}), C–C asymmetric stretching (811 cm^{-1}), O–C=O deformation of the ester group (598 cm^{-1}), rotation of the ester group (490 cm^{-1}), skeletal deformation (373 cm^{-1}), all characteristic of the polyacrylate molecular structure (Refs [29–31]). Furthermore, given the morphology of the B50 target, to study the composition in different regions, we performed Raman spectra in this target over a resin grain (point 1 in Figure 11B) and in the junction region of three grains (point 2 in Figure 11B). The spectrum of the B50 target are acquired at point 1 of Figure 11B (blue) shows boron signals, while the resin signals are strongly attenuated. The spectrum acquired at points 2 of Figure 11B (magenta) shows boron signals, while the resin signals are almost absent. According to these data, the B50 targets appear to be composed of resin grains covered with boron, with a higher content of boron in between the various resin grains.

5.2. Foam coupled boarated targets (ENEA and FBK Institute)

The ENEA and the Bruno Kessler Foundation (FBK) Institutes designed and realized a target by depositing a foam layer on top of an Si–H–B substrate. The foam layer acts as a suitable hydrogen source to increase the contribution of available protons for the $^{11}B(p,\alpha)2\alpha$ reaction.
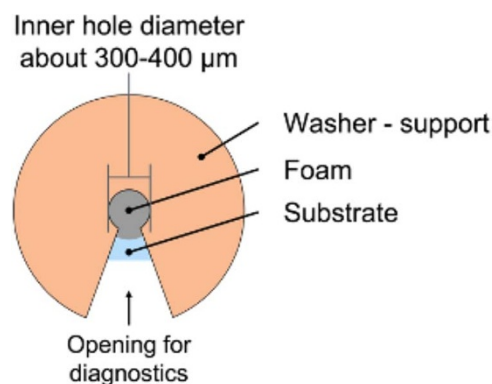

Figure 12. Sketch of the foam target.

These targets have a surface of about 1 cm × 1 cm. The deposited foam layer thickness is around 100 μm and its density ranges from 15 mg/cm^3 to 1 g/cm^3. Figure 12 shows a sketch of these targets with the foam deposited on top and confined by washer support.

5.3. Borated nanoparticles targets (ELI-beamlines)

Hexane nanoparticles (NPs) were synthesized using a Gas Aggregation Cluster Source (GAS) with an RF generator and plasma power settings of 30 and 100 W. At 100 W, NPs with a diameter of 130 nm were obtained, while at 30 W, the diameter increased to 650 nm. Inside the GAS, there was a mixture of argon gas and Hexane in the pressure ratio Ar/Hx=15.7. These NPs were then deposited onto a boron nitride (BN) substrate, resulting in a cumulative NP thickness of approximately 10 μm after 30 minutes of deposition. The unique deposition and production method of these
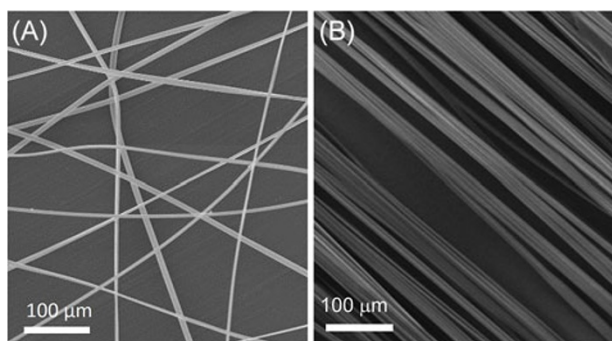
Figure 13. Electrospun fibres obtained by a solution of PMMA in chloroform (375 mg/ml) spun from an 18 G needle. **A.** SEM image of a random field of electrospun fibres, evidencing the good quality of the fibres characterized by absence of beads and ruptures. **B.** Representative SEM image of aligned fibres showing the absence of defects, a good uniformity and general quality of the size and the shape.

NPs resulted in a mesoporous structure with a density of approximately 0.1 g/cm^3. The BN substrate itself has a thickness of 1.5 mm. The hydrogen-rich Hexane NPs are used to accelerate protons from the surface while the BN substrate is used as a source of ^{11}B to enhance the $^{11}B(p, \alpha)2\alpha$ fusion events. These targets are ready and were tested during the first FUSION experimental campaign.

5.4. Targets from University of Salento and IMM-CNR of Lecce

During 2023 the University of Salento and IMM-CNR of Lecce were engaged on the design and the realization of PMMA fibres bundles, characterized by good uniformity and low degree of defects: especially pores (which can lead to missing active material) and beads (which can induce non-uniform density distribution). The activity consisted of the optimization of the fabrication procedure of PMMA fibres, eventually doped by boron, ready to be implemented as potential targets. We have studied two kinds of fibre samples: (a) aligned and (b) randomly oriented fibres (see Figure 13). The starting point is the preparation of the solution in which PMMA is initially dissolved. The optimization process led to fibres with good quality and a high degree of reproducibility. PMMA concentration plays a crucial role, influencing directly the final aspect of the fibres, especially their uniformity and the absence of defects such as pores. By varying the concentration from 100 to 800 mg/ml, we observed different quality of the fibres: too low concentration leads to irregular and broken fibres, whereas the highest concentration leads to inhibition of fibre extrusion from the needle. The ideal concentration is 375 mg/ml, leading to high-quality fibres, uniform and defect-free. In Figure 13, SEM images of the best random (a) and aligned (b) fibres are shown.

5.5. Ammonia borane targets (central laser facility)

Borane ($BnHm$) molecules, which contain high amounts of hydrogen and boron, are promising candidates for proton–boron fusion fuels. One example is diborane (B_2H_6), which has been used as a fusion fuel in magnetically confined plasma experiments (e.g., by TAE Inc.). However, diborane is a flammable and toxic gas, requiring careful handling.

As an alternative, Ammonia Borane (BNH_6), also known as 'AB', has been proposed at the Central Laser Facility (CLF), as a solid, easy-to-handle fusion fuel for laser-driven sources of alpha particles (Ref [32]). AB is a stable powder under ambient conditions,
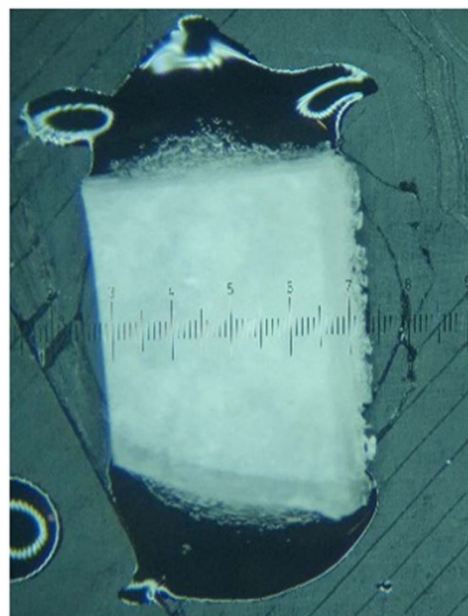

Figure 14. An Ammonia Borane solid target, compressed from powder into 12 mm diameter discs with a thickness of 0.16 mm, was segmented into smaller laser targets. The image shows one of these target segments, highlighting both the edge profile and the typical surface morphology discussed in (Ref [32]).

with a density of 0.78 g/cm^3. This makes it suitable for compression into solid disc-shaped pellets to serve as laser targets. Disc-shaped AB pellets, with a diameter of 12 mm and thickness of 1.2 mm, have been manufactured at the CLF .

Further work was carried out at the FBK, where AB was synthesized and compressed into disc targets, then irradiated with laser pulses to generate alpha particles for the first time (Ref [33]). In this experiment, conducted using the QUB 8 J/pulse, 800 fs laser, a normalized alpha flux of 6×10^7 alphas/J/sr was achieved. This result is comparable to the highest alpha particle yields reported in the literature for laser-driven proton–boron fusion using boron-containing targets. In Figure 14, a microscope image of an Ammonia Borane target.

6. Conclusions

FUSION is the first INFN project funded to study the ICF approach. The project, launched with ENEA and with the participation of many Italian Institutions, will study, in particular, the $^{11}B(p, \alpha)2\alpha$ reaction channel that, even if less energetically favoured with respect to the DT one, presents many interesting and favourable characteristics and represents one of the most promising fusion reaction for the future fusion energy plant.

Conflicts of Interest. The authors declare that there are no conflicts of interest.

References

1. **Belyaev, et al.** (2005) Observation of neutronless fusion reactions in picosecond laser plasmas. *Physical Review E—Statistical, Nonlinear, and Soft Matter Physics* **72**, 026406.
2. **Atzeni S and Meyer-ter-Vehn J** (2004) *The Physics of Inertial Fusion: Beam Plasma Interaction, Hydrodynamics, Hot Dense Matter.* No. 125. Oxford University Press.
3. **Ditmire, et al.** Focused energy, a new approach towards inertial fusion energy. *Journal of Fusion Energy* **42**, 2023.
4. **Craxton, et al.** (2015) Direct-drive inertial confinement fusion: A review. *Physics of Plasmas* **22**, 110501.
5. **Hurricane OA, Zylstra AB and Britcher AL**, **et al.** (2021) Record energetics for an inertial fusion implosion at nif. *Physical Review Letters* **126**, 025001.
6. **Zylstra AB**, **et al.** (2022) Experimental achievement and signatures of ignition at the national ignition facility. *Physical Review E* **106**, 025202.
7. **Abu-Shawareb H, et al.** (2022) Lawson criterion for ignition exceeded in an inertial fusion experiment. *Physical Review Letters* **129**, 075001.
8. **Kritcher AL**, **et al.** (2022) Design of an inertial fusion experiment exceeding the Lawson criterion for ignition. *Physical Review E* **106**, 025201.
9. **Ahmed MW, et al. and Stave S** (2022) Understanding the $^{11}b(p, \alpha)\alpha\alpha$ reaction at the 0.675 mev resonance. *Physical Review E* **106**, 025201.
10. Marvel fusion - the ultimate clean energy solution. https://marvelfusion.com/.
11. Hb11 company. https://hb11.energy/.
12. **Batani K** (2023) Perspectives on research on laser driven proton-boron fusion and applications. *Journal of Instrumentation* **18**, C09012.
13. **Becker HW**, **et al.** (2022) Low-energy cross sections for $^{11}b(p, 3\alpha)$. *Physical Review E* **106**, 025201.
14. **Nevins WM and Swain R** (2000) The thermonuclear fusion rate coefficient for p-^{11}b reactions. *Nuclear Fusion* **40**(4), 865.
15. **Belyaev VS**, **et al.** (2005) Observation of neutronless fusion reactions in picosecond laser plasmas. *Physical Review E* **72**, 026406.
16. **Milluzzo G, et al.** (2023) Extended characterization of alpha particles via laser-induced p-11b fusion reaction in silicon hydrogenated boron-doped thin targets. *Journal of Instrumentation* **18**, C07022.
17. **Consoli F**, **et al.** (2020) Diagnostic methodologies of laser-initiated 11b(p,α)2α fusion reactions. *Frontiers in Physics* **8**, 561492.
18. **Sciscìò M, et al.** (2023) High-sensitivity Thomson spectrometry in experiments of laser-driven low-rate neutronless fusion reactions. *Laser and Particle Beams* **2023**, 1–11.
19. **Margarone D, et al.** (2022) In-target proton–boron nuclear fusion using a pw-class laser. *Applied Sciences* **12**, 1444.
20. **Krus M, et al.** (2024) High yield of alpha particles generated in proton-boron nuclear fusion reactions induced in solid boron hydride $b_{18}h_{22}$. *ArXiv Preprint* arXiv:2407.06729.
21. **Giuffrida L, et al.** (2020) High-current stream of energetic α particles from laser-driven proton-boron fusion. *Physical Review E* **101**, 013204.
22. **Picciotto A, et al.** (2014) Boron-proton nuclear-fusion enhancement induced in boron-doped silicon targets by low-contrast pulsed laser. *Physical Review X* **4**, 031030.
23. Pals laser output parameters. https://www.pals.cas.cz/laser/output-parameters/.
24. **Verona C**, **et al.** Array of time-of-flight diamond detectors for particle discrimination in laser driven p-11b fusion experiments. *Journal of Instrumentation* **8**, 2023.
25. **Consoli F**, **et al.** (2016) Study on a compact and adaptable Thomson spectrometer for laser-initiated ^{11}b(p,α) ^{8}be reactions and low-medium energy particle detection. *Journal of Instrumentation* **11**, C05010.
26. **Salvadori M, et al.** (2023) Univocal discrimination of α particles produced by p(^{11}b, α)2α fusions in laser-matter experiments by advanced Thomson spectrometry. *Laser and Particle Beams* **2023**, 1–12.
27. **Iannin JS** (1978) Solid state communications. *Solid State Communications* **25**, 363–366.
28. **Bykova E, Parakhonskiy G and Dubrovinskaia N**, **et al.** (2011) Experimental pressure-temperature phase diagram of boron: resolving the long-standing enigma. *Scientific Reports* **1**, 96.
29. **Socrates G**, (1995) *Infrared and Raman Characteristic Group Frequencies (3rd edn.).*, Chichester: John Wiley and Sons.
30. **Matsushita A, et al.** (2000) *Vibrational Spectroscopy* **24**, 171.
31. **Nagasawa M Koda S and Nomura H** (1982) *Biophysical Chemistry* **15**, 65.
32. **Turcu ICE, Margarone D, Giuffrida L, Picciotto A, Spindloe C, Robinson APL and Batani D** (2024) Borane (b m h n), hydrogen rich, proton boron fusion fuel materials for high yield laser-driven alpha sources. *Journal of Instrumentation* **19**, C03065.
33. **Picciotto A, Valt M, Molloy DP, Gaiardo A, Milani A, Kantarelou V, Giuffrida L, Nersisyan G, McNamee A and Kennedy JP**, **et al.** (2024) Ammonia borane-based targets for new developments in laser-driven proton boron fusion. *Applied Surface Science* **672**, 160797.